Chin. J. Astron. Astrophys. Vol. 5 (2005), No. 5, 443–447
(*http://www.chjaa.org*)

Chinese Journal of Astronomy and Astrophysics

LETTERS

A New Method of Identifying 3D Null Points in Solar Vector Magnetic Fields *

Hui Zhao, Jing-Xiu Wang, Jun Zhang and Chi-Jie Xiao

National Astronomical Observatories, Chinese Academy of Sciences, Beijing 100012
zhaohui@ourstar.bao.ac.cn

Received 2005 September 6; accepted 2005 September 12

Abstract Employing the Poincaré index of isolated null-points in a vector field, we worked out a mathematical method of searching for 3D null-points in coronal magnetic fields. After introducing the relevant differential topology, we test the method by using the analytical model of Brown & Priest. The location of null-point identified by our method coincides precisely with the analytical solution. Finally we apply the method to the 3D coronal magnetic fields reconstructed from an observed MDI magnetogram of a super-active region (NOAA 10488). We find that the 3D null-point seems to be a key element in the magnetic topology associated with flare occurrence.

Key words: Sun: flares — Sun: corona — Sun: magnetic fields

1 INTRODUCTION

It has been widely accepted that the topological structures of solar magnetic fields are closely associated with magnetic reconnection and hence solar flares and CMEs (Sweet 1969). To understand the magnetic topological structures of the corona, the 3D null-point, which appears to be a vital topological feature in the magnetic fields, should be thoroughly investigated. The definition, classification and properties of the null-point have been theoretically described by Lau & Finn (1990). In analytical form Lau (1993) and Brown & Priest (2001) presented the null-points and associated topological structures in their models. Comparing the topological sketches and observations, Filippov (1999), Aulanier et al. (2000) and Fletcher et al. (2001) identified the null-points in corona. A general and direct method, independent of analytical models and topology sketches, has been suggested by Wang & Wang (1996) for 2D vector magnetic fields. Inspired by this work, we develop a method (from the Poincaré-Hopf theorem in differential topology) which can identify 3D null-points directly in any given 3D vector field.

* Supported by the National Natural Science Foundation of China.

2 THEORY AND METHOD

Suppose $V(M)$ is a continuous vector field on a space M, $p \in M$ satisfies: $V(p) = 0$ and there exits a neighborhood $U(p)$, $V(U \setminus \{p\}) \neq 0$. We say p is an isolated singular point (or null-point) in $V(M)$. Generally, in an actual vector field, we need a method by which we can identify the null-point through studying the behaviors of vectors based on its neighborhood $U \setminus \{p\}$. In the global differential topology, the Poincaré index can meet with this requirement.

Suppose that M and N are oriented differential manifolds with the same dimension, $p \in M$ and $q \in N$. Let f be a local differentiable homeomorphism from $U(p)$ into $U(q)$, φ and ψ are local coordinate systems (in Euclidean spaces) have positive orientation in $U(p)$ and $U(q)$, respectively. Define (this definition does not depend on the choice of φ or ψ)

$$\operatorname{sgn}(f_{*,p}) = \operatorname{sgn}(\det(\mathbf{D}(\psi \circ f \circ \varphi^{-1}))_{\varphi(p)}), \tag{1}$$

where $\mathbf{D}$ is differential of a mapping. If f is a smooth map, M and N are compact smooth manifolds and $y \in N$ is a regular value of f (that is to say, for any $p \in f^{-1}(y)$, $\operatorname{sgn}(f_{*,p}) \neq 0$, or $f^{-1}(y)$ has no definition) we called

$$\deg(f, y) = \sum_{p \in f^{-1}(y)} \operatorname{sgn}(f_{*,p}) \tag{2}$$

the oriented mapping degree of f at y. When N is connected, $\deg(f, y)$ is a constant at every regular value $y \in N$. This constant is called the oriented mapping degree of f, denoted by $\deg(f)$.

For example, let $M = N = S^1$ ($S^1 = \{(x, y) \in \Re^2 \mid x^2 + y^2 = 1\}$), and the positive orientation be anti-clockwise (Fig. 1). Along M, $f(M)$ (a closed curve) might go to and fro in N. For seeing more clearly, we illustrate $f(M)$ outside N in Figure 1. At each point which is mapped to the inflexion of $f(M)$ by f, the Jacobi determinant, $\det(\mathbf{D}(\psi \circ f \circ \varphi^{-1}))_{\varphi(p)}$, should be zero. Except these four inflexions, any $y \in N$ is regular. For any regular value y, $\deg(f)$ always be $+1$ in this example. In the condition of $\dim M = 1$, the number of $\deg(f)$ implies how many circles $f(M)$, a closed curve, rotates around N in positive orientation.

Let M ($\dim M = n, n = 1, 2$) be a compact boundless smooth manifold and f a continuous map : $M \to \Re^{n+1}$. For any $z \in \Re^{n+1} \setminus f(M)$, we can define another continuous map

$$\theta : M \to S^n, \tag{3}$$

$$x \mapsto \frac{f(x) - z}{\|f(x) - z\|}. \tag{4}$$

The oriented mapping degree of θ is called the winding number of f around z, denoted by $W(f, z)$. Notice there is a natural orientation on S^n induced by its outer normal.

Suppose G is an open subset of $\Re^n$, V a continuous vector field on G, and $p \in G$ an isolated singular point of V. Select a number $\epsilon > 0$, such that the ball $D_{p,\epsilon} \subset G$, centered at p with radius ϵ, has no other singular point of V in $D_{p,\epsilon}$ except p. We define the index of V at p to be

$$\operatorname{ind}_p V = W(V \mid S_{p,\epsilon}, 0), \tag{5}$$

where $S_{p,\epsilon} = \partial D_{p,\epsilon}$. Also in Figure 1 we can choose M ($\dim M = 1$) as $S_{p,\epsilon} \subset G$, $V \mid S_{p,\epsilon}$ presented by arrows, such that $f(M)$ is just the normalization of $V \mid S_{p,\epsilon}$ (remember $f(M) \subset N$). We have known that in this example, index = $\deg(f) = +1$, hence there must exist a singular point in $D_{p,\epsilon}$. Wang & Wang (1996) have shown some familiar 2D singular points with index = 0 or ± 1. The indexes imply how many circles the normalized image of $V \mid S_{p,\epsilon}$ rotate around S^1 in positive orientation. We can measure the angle of every two adjacent vectors and

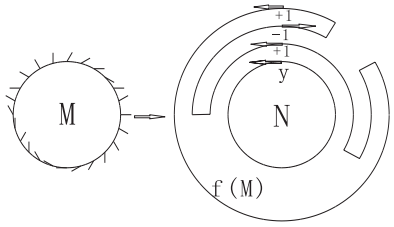

Fig. 1 An illustration of the theory in 2D. Vectors on M are shown in short lines, and $f(M) \subset N$ is placed outside N . The positive orientation of N and the signs of three bifurcations at regular value $y \in N$ are marked by arrows and numbers.

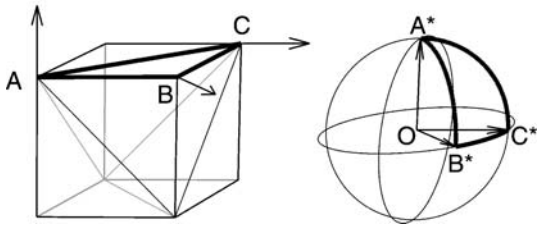

Fig. 2 An illustration of the theory in 3D. Vectors at A, B and C on cube vertex and their images A^*, B^* and C^* on S^2 are shown in arrows. $\triangle ABC$ and corresponding spherical triangle are marked by bold sidelines.

integrate these angles along M. Divide the integral by 2π and we obtain the index finally. It is the same in the 3D case. In Figure 2, we choose a little cube's surface as the closed manifold, M ($\dim M = 2$), including a point that we examine. Normalize the vectors at the cube's vertex and translate these images of vectors to S^2 ($S^2 = \{(x, y, z) \in \Re^3 \mid x^2 + y^2 + z^2 = 1\}$), integrate these twelve spherical triangles on S^2 and divide the integral by 4π. Then we obtain the index which tells us how many times the image of vector field wraps S^2 in positive orientation.

3 APPLICATION

3.1 A Test by an Analytical Model

We first use our method to search a known null-point of the analytical model suggested by Brown & Priest (2001). There exist three negative sources of equal magnetic strength, $\epsilon_S = -1$, at $(0, 1, 0)$, $(\cos\frac{7}{6}\pi, \sin\frac{7}{6}\pi, 0)$, $(\cos\frac{11}{6}\pi, \sin\frac{11}{6}\pi, 0)$ and one positive source of unit strength in the center of the triangle (the contours are shown in Fig. 3). The analytical solution gives a null-point at $(0, 0, 0.962)$. In the $[-2, 2] \times [-2, 2] \times [0, 3]$ box (Fig. 3), we sum up the values of 12 spherical triangles in each little cube (Fig. 2) composed of eight pixels. If a cube has no singular point its index should be equal to zero. In the box we find that the only one cube with index equal to -1 contains the null-point that we have known by the analytical solution, while for all others the index is equal to zero. The topological structure is shown in Figure 3. A separatrix dome separates the half space $z > 0$ into two independent topologies (these are marked with different colors). Moreover, the spine on the z-axis crosses the 3D null-point at the peak of the dome.

3.2 Applying the Method to an Active Region

We also applied the above method to search for null-points in extrapolated magnetic fields of the solar active region (AR), NOAA 10488. It is one of the three super-active regions that appeared in the interval October 18 to November 4, 2003. These three ARs produced many unexpected eruptive events (Zhang et al. 2003). Figure 4 shows a series of photospheric vector magnetograms of the AR NOAA 10488. This region began to emerge on October 25 and grew rapidly to a large AR on October 27, then reached its decay phase when approaching the west edge of the sun on November 3. The AR produced several flares and CMEs during its passage over the suns disk. On October 30, the 1F/M1.6 flare which we consider in this work began at 01:56 UT, reached its maximum at 02:07 UT and ended at 02:29 UT. In this fast growing active

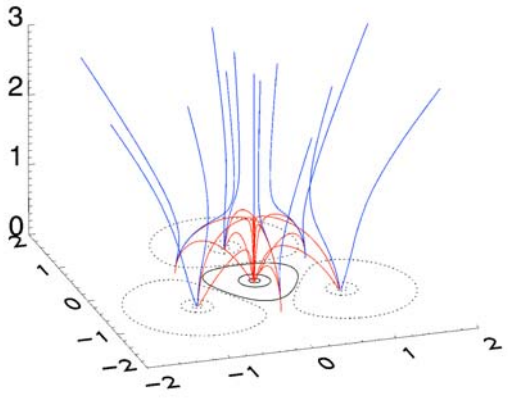

Fig. 3 Magnetic topology structure of the analytical model. Contours on the $z = 0$ plane is longitudinal magnetic filed. Positive and negative fields are shown in solid and dashed lines, respectively. A dome divides the region $z > 0$ into two different parts shown in red and blue. A 3D null point exists at $(0, 0, 0.962)$.

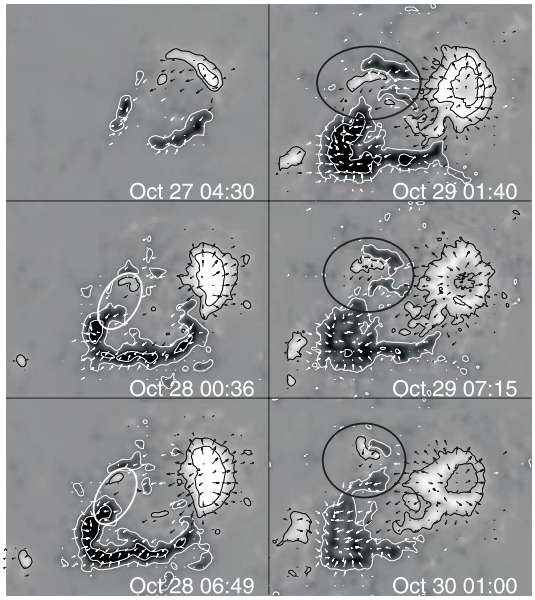

Fig. 4 Time sequence of photospheric vector magnetograms of AR 10488. Gray maps and contours in the figure present the longitudinal magnetic fields. Arrows show the transverse magnetic fields with length proportional to field strength.

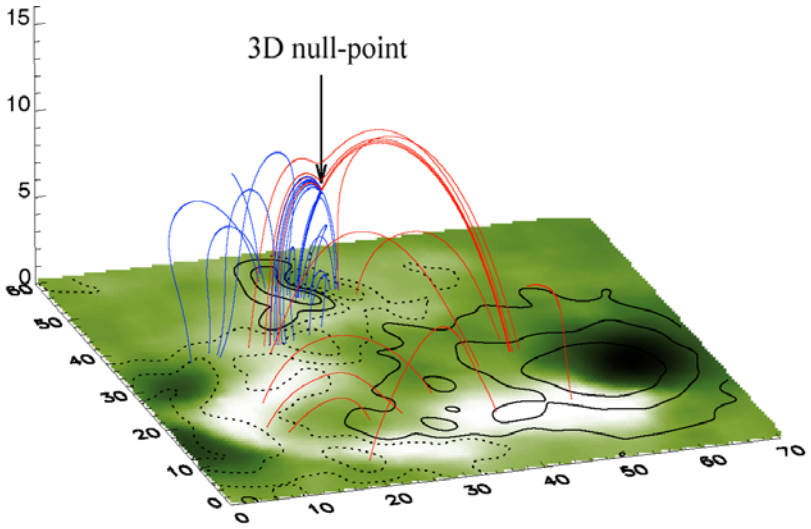

Fig. 5 Linear force-free field lines, reconstructed from the MDI magnetogram of 2003 October 29, 22:23 UT, in units of MDI pixels (2.0″). The background is Huairou Hα image of 2003 October 30, 02:02 UT. Contours of the vertical component of the positive and negative fields are shown in solid and dashed lines, respectively. The spine is a curve from one positive source to another. A dome-like surface divides the region $z > 0$ into two parts. The field lines inside the dome are shown in blue, and those outside, in red. A 3D null point exists at $(31.2, 47.4, 6.2)$.

region, we noticed that the positive flux belonging to an emerging flux region (EFR) (framed in white oval), was gradually surrounded by several negative sources (Fig. 4). Because the sum of the negative fluxes locally outweighs the positive flux, a null point might be present above the region framed with a black oral in Figure 4 (Brown & Priest 2001). We use the linear force-free extrapolation method with a constant α suggested by Seehafer (1978) to obtain the 3D vector magnetic fields. The boundary condition is taken from MDI magnetogram and the value of α is obtained from the Huairou vector magnetograms for the nearest time. As expected, we found a null-point above this AR. Figure 5 shows that the field lines near this null-point are very similar to those given by the analytical model of Brown & Priest (see Fig. 3). Some magnetic lines of force which anchored within two flare ribbons pass through the vicinity of the 3D null-point or have some relations with the spine and fan structures associated with the null point (Fig. 5). Different from the analytical model, the spine is a curve from one positive source to another, while the fan structure is dome-like and asymmetric. The null-point, where the spine crosses through the dome, is at the height of $12''$ (8700 km) above the solar photosphere.

4 DISCUSSION AND CONCLUSIONS

Undoubtedly null-points in coronal magnetic fields are vital topological features for understanding coronal phenomena. In this work we present a theoretically-conceived method of searching for 3D null-points and apply this method, for the first time, to identify a 3D null-point in coronal magnetic fields. As a test we use this method to search for a known 3D null-point in the analytical model of Brown & Priest (2001). Applying the method to AR 10488 we find there is some association between solar flare and 3D null-point. This case also presents a good instance of showing why regions with so-called δ spots are likely to produce flares (Brown & Priest 2001). With the 3D Poincaré index we can indeed extend the early work (Wang & Wang 1996) to 3D vector magnetic fields in corona. However, using eight points instead of a closed surface might be too rough when the vector field is complex in terms of the grid scale. These closed surfaces should not be so big as to have the probability of including more than one singular point, otherwise the method may not work. For comprehensively studying the relations of magnetic topology and solar activity, we would construct all kinds of topology structures which would produce 3D null-points and related features. We would also detect singular lines and singular surfaces, and practically track these topology features in the magnetic field evolution that lead to explosive activities in the corona.

Acknowledgements The work is supported by the National Natural Science Foundation of China (Grant 10233050) and National Key Basic Research Science Foundation (G2000078404). We thank Cheng Zhou for providing the extrapolation code and Chao Liang for her help.

References

Aulanier G., DeLuca E. E., Antiochos S. K., McMullen R. A., Golub L., 2000, ApJ, 540, 1126
Brown D. S., Priest E. R., 2001, A&A, 367, 339
Filippov B., 1999, Solar Phys., 185, 297
Fletcher L., Metcalf T. R., Alexander D., Brown D. S., Ryder L. A., 2001, ApJ, 554, 451
Lau Y. T., 1993, Solar Phys., 148, 301
Lau Y. T., Finn J. M., 1990, ApJ, 350, 672
Seehafer N., 1978, Solar Phys., 58, 215
Sweet P. A., 1969, ARA&A, 19, 163
Wang H. N., Wang J. X., 1996, A&A, 313, 285
Zhang H. Q., Bao X. M., Zhang Y. et al. 2003, Chin. J. Astron. Astrophys., 3(6), 491